TESTING AND MODELING OF FAILURE BEHAVIOUR IN FIBER METAL LAMINATES

J. Sinke*, H. de Boer, P. Middendorf*****
*TU Delft, NL **Advanced Lightweight Engineering, Delft, NL *** EADS Corporate Research Center, Ottobrunn, G.

Abstract

Fiber Metal Laminates (FML) are hybrid materials consisting of alternating layers of thin metal sheets and composite layers. GLARE is the best known example of these laminates and is applied in the Airbus A380. The main incentive for the development of these hybrids is their excellent Damage Tolerant behavior when compared to metal alloys. When compared to composite materials, FML offer some plasticity and can be manufactured applying simple (metal) manufacturing processes.

The laminates, due to their composition, fail in modes, different from the ones for monolithic metals and full composites. Metals fail in a more or less ductile manner, composites fail by failure of the fibers and/or (subsequent) fracture of the matrix and fiber-matrix interfaces.
The different constituents involved in FML, may each fail in their own failure mode: fibers in breaking, the adhesive in shear or in peel, and the metal in ductile fracture or local buckling. Assembled in a laminate also coherence failures may occur, like delamination, which occur at the interfaces between the metal and the composite layers. This delamination is induced by tensile, compressive or bending stresses, and results from high tensile and shear stresses at the interfaces.

This paper discusses some experimental and numerical results of an ongoing research focused on the failure behavior of FML, and of GLARE in particular. This research is performed in a Specific Targeted Research Project under the 6th Framework of the European Commission, called DIALFAST [1],

in a Work package about micro-mechanical modeling of FML. The work in this WP was performed by Airbus, TU Delft and EADS CRC; ALE was subcontracted by Airbus.

The main objective for this work package is to develop FE-models that can predict adequately the failure of typical details in FML structures like joints, splices, etc. The models are developed to describe the failure behavior observed during the experiments and are validated with the measurements from these tests.
The FE-models, as described in the paper, are used to develop design tools for the design of FML structures and to predict and describe the failure of structures and structural details in GLARE. The macro-mechanical testing and modeling is part of another Work package within the DIALFAST program.

Two examples of failure, investigated during the research, are described in this paper: delamination of laminates and the failure of riveted joints.

1 Introduction

Fiber Metal Laminates (FML) are made of alternating layers of thin metal sheets and composite layers. The layers are adhesively bonded using the matrix material of the composite layer. The FML concept result in a wide range of different laminate, since the three main components or ingredients, the metal alloy, the fiber system and the matrix or resin, are variables. This range is further increased by variation in the build-up of the laminates by

variables like the thickness of the layers, the number of layers, the fiber orientation, etc.

Figure 1. Example of a FML (GLARE 2-3/2-0.4)

An example of a FML is presented in figure 1. The particular FML is GLARE 2-3/2-0.4. This laminate is made of the Aluminum 2024-T3 alloy, and of UD-prepregs consisting of S-glass fibers embedded in a FM94 epoxy resin. In this particular laminate each composite layer is made of two UD-prepreg layers or –plies. All plies are oriented in the same direction, resulting in a Uni-Directional (UD) laminate. The laminate has five layers: three metal layers (each 0.4 mm thick), and 2 composite layers. For the metal layers the most common thickness is 0.4 mm; the thickness of a composite layer depends on the thickness and number (2 to 4) of used prepregs. The thickness of the composite layers of the presented GLARE-2 laminates is 0.25 mm.

A brief history of the development of FML [2]

FML are related to the bonded structures Fokker introduced in the 1950s for its F-27 aircraft. Since then the bonding technology improved over the years and in the 1970s research was performed towards fiber reinforced bonded structures. At the end of that decade the Technical University took the lead and presented the first Fiber Metal Laminate, named ARALL in 1979. The acronym ARALL stands for: ARamid ALuminum Laminate, which is a FML based on aramid fibers.

From the early '80s onwards, the research on the laminates expanded and was sponsored by interested companies like ALCOA(US) and AKZO (NL). The first large application for ARALL material was the cargo-door of the C17 military transport aircraft. Although the performance of this cargo-door was good, the door was replaced later by a metal one for cost reasons.

In 1986 a new type of FML was introduced: GLARE, based on glass fibers. In this FML the aramid fibers have been replaced by glass fibers. The reason for this change was the fact that at some load cases the aramid fibers failed. Fiber failure is unacceptable, because this jeopardizes the crack-bridging, and thereby the most important asset of FML: the excellent fatigue resistance. Glass fibers don't fail during fatigue, and GLARE became the most important variant for FML.

An important milestone in the development of GLARE was the solving of the scaling problem by so-called "splicing" of the metal layers (see figure 2). Applying this concept, very large skin panels can be manufactured without the need of (riveted) joints. These panels are made using composite technology: the large skins (and doublers) are made by lay-up processes. The "splicing" was a big improvement since in the ARALL-period the laminates were treated as metal sheets: the laminates were made flat, and subsequently formed and joined into large structures. This resulted in more riveted joints (and weight) and was complicated since the formability of the laminates is poor.
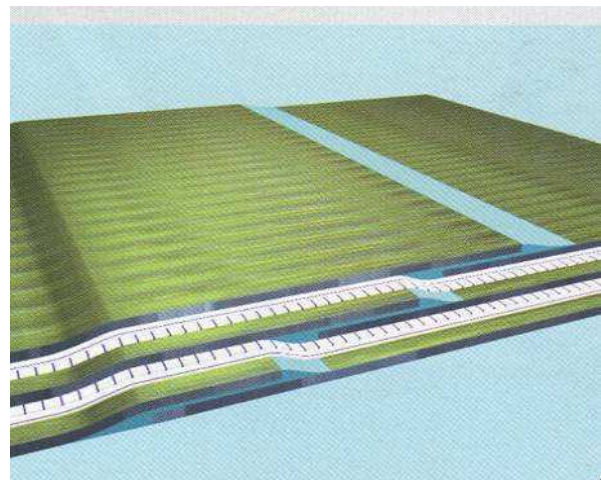
Figure 2. Example of a splice in a FML

In the 1990s Airbus started the development of a very large passenger aircraft. This aircraft should extend the available capacities of aircraft offered to customers. The design was released in 1996, and designated as "A3XX". GLARE was regarded as a potential candidate material for the aircraft fuselage As a result the research and development activities at the University of Delft, the National Aerospace Laboratory and Stork Fokker, increased significantly. The Dutch government supported the research. The main objective of the research was to assure the readiness of GLARE for application in large structures like the Airbus A3XX. The final result is that GLARE laminates are applied in a significant part of the A380 fuselage (see figure 3). Most of these skin panels are produced by Stork Fokker AESP at their Papendrecht plant. Other applications of GLARE laminates are the leading edges of the tail planes of the A380.
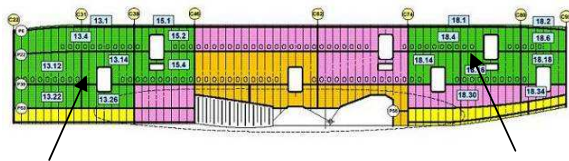
Figure 3. GLARE-panels in the Airbus A380

Characteristic features of FML

FML like GLARE are specifically developed as fatigue resistant materials. The fatigue resistance is due to the crack-bridging of the fibers (see figure 4). When the laminate is subjected to fatigue loads crack will initiate in the metal layers, but the fibers in the composite layers will bridge and retard the crack growth: The bridging of the crack reduces the stress intensity at the crack tip. This result in crack growth rates which are one or two orders of magnitude smaller than for aluminum alloys.

Other typical features that are important are:
- high residual strength. The Damage Tolerance of FML could be high: depending on the composition, it can sustain high loads in damaged condition. The ductility of the metal

constituents and the failure behavior of the laminates, are contributing to this DT-property.
- high impact and blast resistance. The impact resistance of FML is better than for aluminum alloys and full composites. The laminates absorb energy by plastic deformation (metal behavior) and by membrane stresses (composite behavior). For the blast resistance the "strain hardening" of FML is important: the high strain hardening coefficient results in the distribution of the impact energy over a large surface area.
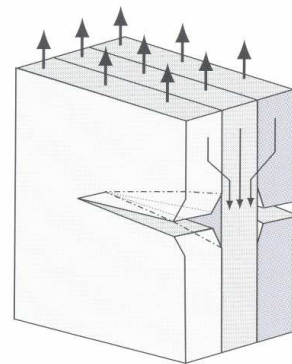
Figure 4. Fiber bridging in FML.

- high corrosion resistance. The layered structure of FML is beneficial for the corrosion and absorption properties of the laminate. The composite layers protect the internal metal layers from corrosion; the metal layers protect the composite layers from moisture uptake and Ultra Violet radiation.
- high flame resistance. The flame resistance of FML is based on carbonization of the first composite layer and the delamination of the remaining layers. Both effects prevent of retard the flame penetration of a skin material and often the aluminum alloy contributes with rapid heat dissipation due to its high thermal conductivity.
- has some ductility. The overall ductility of FML, due to the metal constituent, is beneficial for all locations with stress concentrations. The plastic deformation will relieve the peak stresses and prevent or postpone premature failure.

Among the less favorable properties are the limited stiffness of the laminates, the limited manufacturing capabilities and the high material costs (although fabrication of integrated panels can lead to competitive substructures).

2 Failure Behavior of Fiber Metal Laminates

Fiber Metal Laminates are materials composed from different materials: the metal sheets and the composite layers; the latter consisting of fibers and a matrix material. Between the fibers and the matrix and between the composite and metal layers there are interfaces where the matrix material adheres to the fibers and the metal sheet.

This laminate composition may introduce a number of different failure modes:

- yielding of the metal layers. As for metal alloys the yielding is a limit for the derivation of design allowables: yielding is not acceptable during daily life. However, yielding also offers stress redistribution in case excessive loads, and thereby results in a safer structure. Just like metal alloys, FML show a stress strain curve with a yield point: the curve is bilinear with a clear transition from elastic to plastic deformation.
- A second failure mode related to the metal constituent is the cracking of a metal layer. Although by in-plane deformations the fibers fail first, by bending the outer metal layer may fail. In the case the outer layer cracks by exceeding the failure strain of the metal. Also cracking by fatigue is an example of this failure mode in metal.
- fiber failure. Fibers deform elastically until failure. The plastic or permanent deformation is negligible. The fibers are the reason for the limited failure strain of the FML: in the range of 1 -4 %, depending on the selected fibers. When, i.e. during a tensile test, the limit strain of the fibers is exceeded, the fibers fail by breaking, resulting in the subsequent failure of the laminate. This failure can be rather "explosive": the released elastic energy of the fibers causes significant damage to the laminate: delamination and metal failure.

- matrix cracking. Matrix cracking occurs when the maximum strain of the matrix material is exceeded. Since, the matrix of the laminates is full with stress concentrations, matrix failure is a local phenomenon, although it happen as wide spread cracking. This failure mode in itself is usually not the cause for laminate failure. Nevertheless, matrix cracking is detrimental for durable application of FML.
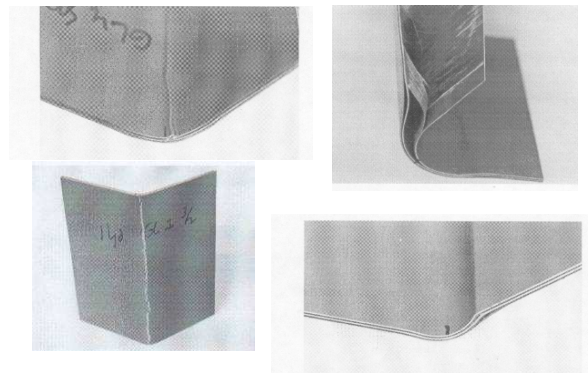
Figure 5. Some basic failure modes of FML. (clockwise starting at top-left: buckling of a metal layer, edge delamination, delamination close to a bend zone, cracking of metal layer).

Besides these constituent failures, there are also a few failures related to the composition of the FML.

- The delamination of fiber and matrix. This type of delamination is the most common one, since this is the weakest link. If during testing, i.e. during fatigue, some delamination occurs, the bonding between the fibers and the matrix fails.
- The delamination of composite layer and metal layer. This type of delamination at macro-level can be attributed to the failure of the fiber-resin bond. The failure of the bond between the resin and the metal layers (including the pretreatments) is rare.
- The last failure that may occur is the local buckling of a metal layer. During bending when the inside layer is loaded in compression, this layer may delaminate and

buckle. This happens only is case of thin metal layers (thickness of 0.3 mm or less). Some failure modes are presented in figure 5.

3 Testing of FML

During the research and development of FML for the A380, a large number of tests have been performed, both in numbers as well as in different specimen. Many of these tests have been reported, including the associated models, in papers and reports (including PhD-thesis). To mention a few: Testing and modeling of static properties, also at elevated temperatures, by Hagenbeek [3], Bearing behavior of FML at joints by Van Rooijen [4] and crack growth behavior of FML by Alderliesten [5].

In this paper the focus is on the fracture energy testing and the testing of riveted joints.

Fracture of an interface may occur in different fracture modes. In Figure 6 the three different fracture modes are presented: Mode I (a tensile type of fracture), Mode II (in-plane shear type), and Mode III (out-of-plane shear type). During the research Mode III was not tested, instead a Mixed Mode of Mode I and II has been tested.
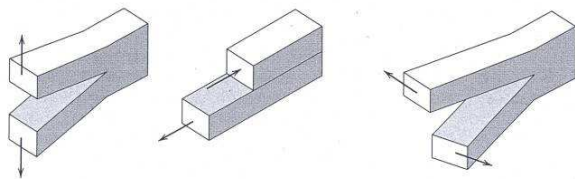
Figure 6. The three principal fracture types: Mode I, Mode II and Mode III. (from left to right).

Mode I
In Mode I, the test specimen is loaded by peel forces, and the fracture is a tensile type of fracture of the interface. For determination of a quantitative value of the fracture energy of the interface, the load and displacement are recorded during the test. From the Load-displacement plot the fracture toughness energy of the interface (G_{Ic}) is calculated (see below).

The used specimen has a geometry similar to the specimen for composite materials, except for one significant modification. During the test only elastic deformations are allowed in the two separating parts. FML contain metallic layers, and plastic deformation of the metal layers may occur, which would result in unreliable test data. In order to obtain proper test data, 4.0 mm thick adherents (Al-7075-T6 alloy) are bonded onto both sides of the specimen.
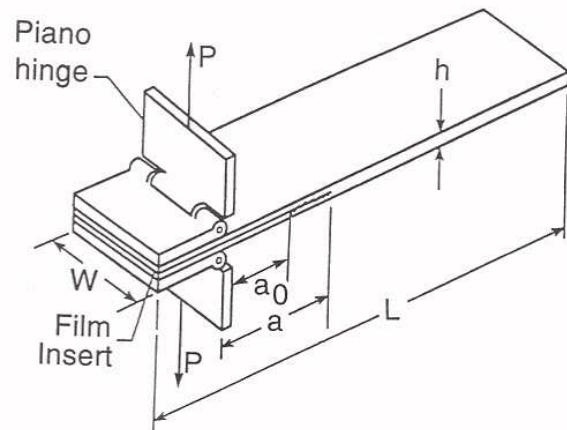
Figure 7: Test (top) and test specimen (bottom) for Mode I testing.

In figure 7 a picture of the test and the geometry of a mode-I test specimen are presented. The dimensions of the specimen are: length (L), width (w), and thickness (h).

By pulling at the piano hinges the prefabricated crack will propagate through the specimen. Before the actual test run, a sharp starter crack of about 10-15 mm is created, originating from the artificial crack made by a Teflon-insert. The artificial crack (a_0), and the crack extension is equal to the starter crack (a).

During testing the applied force (P) decreases steadily (see figure 8) – but the fracture energy is assumed to be constant over the interface.

Using the load-displacement curve the interlaminar fracture toughness energy G_{IC} can be calculated by the following procedure:
- Determine the total energy required to create the crack by measuring area A in figure 8.
- Divide the energy by the width of the specimen (w) and the crack extension (Δa).

The value of G_{IC} (in J/m^2) becomes:

$$G_{IC} = \frac{A \times 10^6}{\Delta a \times w} \qquad (1)$$

G_{IC} *the fracture toughness energy [J/m^2]*
A *energy [J] to achieve the total propagated crack length – see figure 8*
Δa *the propagated crack length [mm] – see figure 8*
w *width of the specimen [mm]*
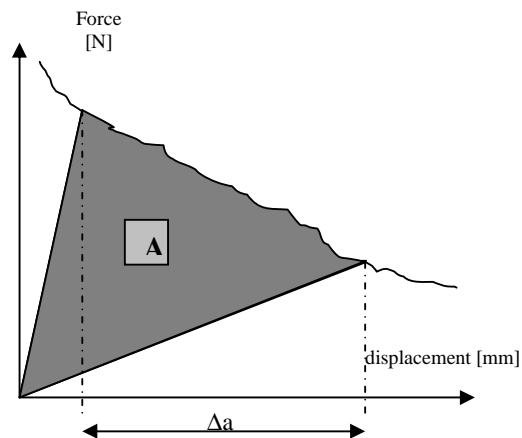
Figure 8. Schematic presentation of the determination of the fracture energy A.

Mode II
In Mode II the test specimen is loaded by shear stresses, introduced by a bending moment. The fracture of the interface occurring during this test is an in-plane shear fracture. For the determination of a quantitative value of the fracture energy of the interface, the load and displacement during the test are recorded. Using the maximum Load from the plot the fracture toughness energy of the interface (G_{IIc}) is calculated.

Again, in order to prevent plastic deformation of the metal layers in the FML, thick adherents (Al-7075-T6 alloy) are bonded onto both sides of the test specimen.
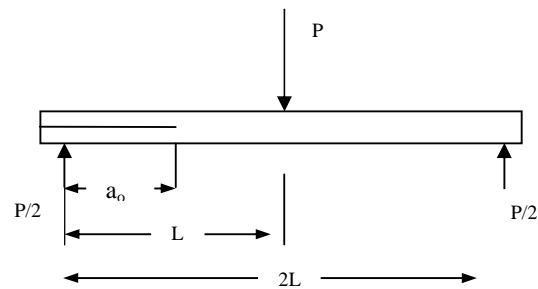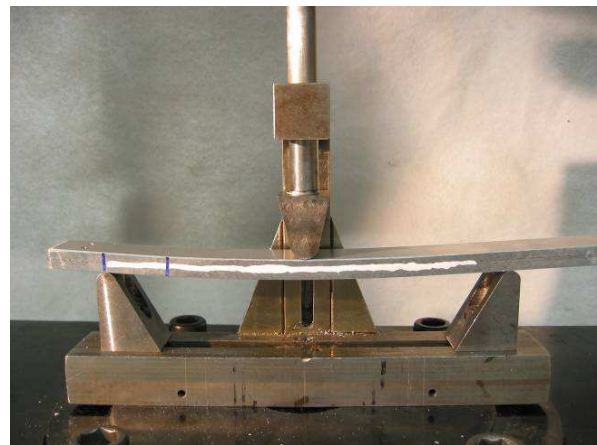
Figure 9. Test (top) and specimen geometry for the Mode II test.

A simple sketch of the test and the specimen geometry is given in figure 9. In this figure the length of the pre-crack is described by the parameter a_0. The specimen is loaded in a three point bending mode, applying a load P in the centre, and using a span length of 2L.

For the measurement of the fracture toughness energy in Mode II, a pre-cracked specimen is loaded to a critical load P. At load P the crack

starts propagating in a unstable manner. The value of the fracture toughness energy G_{IIC}, is related to this maximum load and some geometrical parameters.

So the G_{IIC}-value (in J/m^2) becomes:

$$G_{IIC} = \frac{9P \times a^2 \times d \times 1000}{2 \times w \times (0.25L^3 + 3a^3)} \qquad (2)$$

G_{IIC} *the fracture toughness energy [J/m^2]*
a   *initial crack length – see figure 9 [mm]*
P   *critical load to start the crack [N]*
d   *crosshead displacement at the moment of crack delamination onset [mm]*
w   *width of the specimen [mm]*
L   *span length – see figure 9 [mm]*

Mixed mode.
The third type of tests within DIALFAST is the Mixed Mode test; a Mode in which the interface is loaded with peel and (in-plane) shear forces.
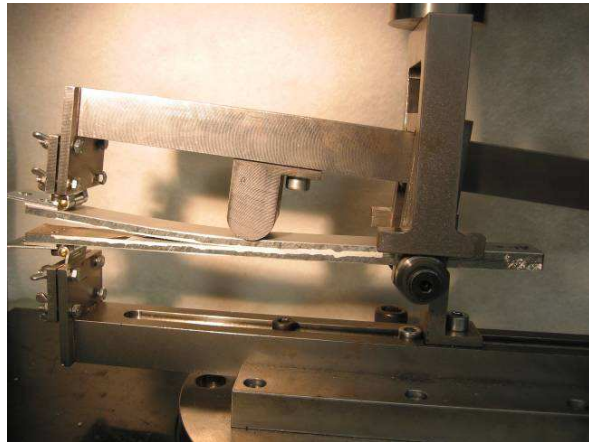
Figure 10. Test (top) and test set-up (bottom) for the Mixed Mode test.

For the test series a 1 to 1 ratio (50/50) between the Mode II and Mode I is selected. This ratio determines the values of the span length (L) and the variable (c) – see figure 10 according to equation 3 (for c ≥ L/3).

$$\frac{Mode \cdot II}{Mode \cdot I} = \frac{3 \times (c+L)^2}{4 \times (3c - L)^2} \qquad (3)$$

The test is recorded with a Force-displacement curve, like the Mode II test. Again, depending on the Mixed Mode ratio, instability of the fracture may occur.

The fracture energies can be retrieved from the following formulas:

$$G_{IC} = \frac{12 \times a_0^2 \times (3c - L)^2 \times P^2}{16w^2 \times h^3 \times E_{11} \times L^2} \qquad (4)$$

$$G_{IIC} = \frac{9 \times a_0^2 \times (c + L)^2 \times P^2}{16w^2 \times h^3 \times E_{11} \times L^2} \qquad (5)$$

G_I, G_{II} *the fracture toughness energy [J/m^2]*
E_{11} *Elastic modulus in longitudinal direction of specimen[MPa]*
a_o *initial crack length [mm] – see figure 9, 10*
P   *critical load [N] to start the crack*
δ *crosshead displacement [mm] at onset of crack delamination*
w   *width of the specimen [mm]*
L   *span length [mm] – see figure 9, 10*
c   *lever length [mm]*
h   *half thickness of the specimen [mm]*

Rivet strength testing.
In addition to the fracture energy tests also rivet strength tests have been performed and modeled. The rivet strength has two values: a bearing yield and a bearing ultimate strength. The tests are performed on anti-symmetric specimen and can be regarded as the coupon tests, required to model the strength of riveted joints.

The test cycle involves a reloading loop in order to obtain the right value of the bearing yield,

which is specified as the yield strength at 2% ovalisation of the rivet holes.

By unloading and reloading the right value of the secondary modulus is obtained, which can be used for the determination of the bearing yield strength. This is presented schematically in figure 11.
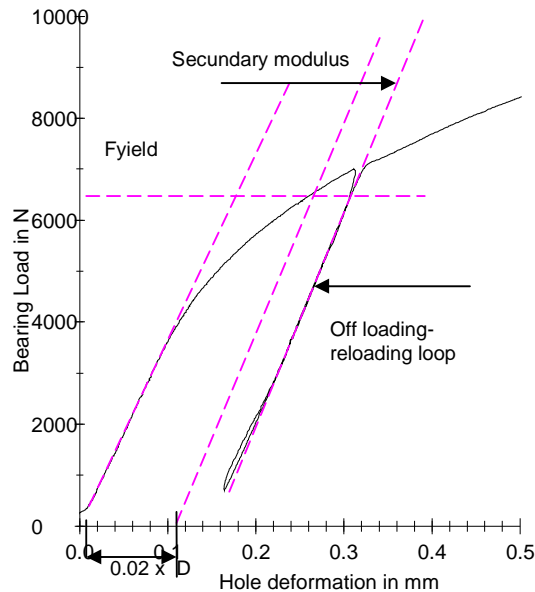
Figure 11. The cycle to determine the bearing yield strength.

The ultimate bearing strength is directly related to the maximum load during the test.

4 Finite Element Analysis of FML

In order to benefit from the advantages of innovative FML versions, the design engineer must be able to predict the failure behaviour of the FML as described in a FE analysis.

For this purpose, proper constitutive relations have to be developed, taking into account the relationships of the materials involved and providing a detailed simulation capability of the damage behaviour until failure.

The simulations are performed on two levels: microscopic models for individual constituents, cross-sections and failure mechanisms, and macroscopic models, i.e. shell-like elements, for structural details. The micro-modelling is presented in this paper.

The micro-mechanical approach is used in the modelling of riveted joints, and in the next paragraph the numerical results are compared with some experimental test data.

The choice to model the individual layers or plies separately leads to a uniform approach for all FML types possible. Still, the number of elements used is relatively small. This choice implies that both the aluminum layer and the prepreg layer are considered as homogeneous materials with given constitutive parameters. In particular, orthotropic material properties are given to the prepreg.

Usually, the adhesive bonding between the aluminum and the prepreg surfaces is of excellent quality, and the interface strength is much higher than the strength in the transition zone between fiber rich and resin rich zones of the prepreg [7]. Delamination will therefore start in this zone. Experiments have shown that delamination may also grow in the resin rich zone between two plies, so particular attention must be paid in modeling the interface between mated plies. In principle, different methods can be applied to model this area:

- by means of an additional layer of continuum elements
- by lumping the behavior of the layer in zero-thickness interface elements
- by interaction surfaces.

The first approach leads to a large number of elements, and the second method implies congruent meshes of the two adjacent plies, and therefore the interaction surface method was chosen to be implemented in ABAQUS.

Damage modeling

Damage in FML can be divided in damage in the aluminum, damage in the prepreg and delamination – see chapter 2.

For the aluminum a smeared crack model was introduced including alignment of the stress-strain relation with the axis of orthotropy (cracking) and reduction of normal and shear

stiffnesses. For the analysis of joints, the rivets are modeled using the same approach.

For damage in the prepreg, a distinction is made between the matrix failure and the fiber failure. Both are implemented in the models by the ABAQUS user subroutine UMAT.

Delamination between two layers may take place when a failure criterion (see below) has been exceeded. Delamination is implemented by the user subroutine UINTER.

Fibre/matrix failure

Fiber or matrix failure only occurs inside a prepreg layer. Matrix failure is a non-fatal failure mode.

A laminate will show stress redistributions after first ply cracking and additional loading of the laminate is still possible [8]. For a correct description of a laminate structure also the effects of crack propagation have to be described that influences the material properties of the cracking ply. For a finite element modeling on a meso-level, the degradation of the properties at a ply level is needed. The failure criterion used here is a stress-based continuum damage formulation with different failure criteria for matrix and fiber failure. A gradual degradation of the material properties is assumed. This gradual degradation is controlled by the individual fracture energies of matrix and fiber, respectively.

The user-subroutine UMAT is used for implementation of the damage model. For matrix failure the following failure criterion is used:

$$f_m = \sqrt{\left(\frac{\sigma_2}{\sigma_{2,\max}}\right)^2 + \left(\frac{\tau_{12}}{\tau_{12,\max}}\right)^2} \qquad (6)$$

$\sigma_{2,\max}$ *maximum stress $\perp$ to the fiber direction (evaluated separately for tension/compression)*

$\tau_{12,\max}$ *the shear failure stress*

f_m *failure occurs when $f_m > 1$.*

When damage occurs, a damage parameter is calculated:

$$d_m = \frac{1}{f_m} e^{\left(-\sigma_{2,\max}(f_m-1)/(C_{22}\,G_c)\right)} \qquad (7)$$

Similarly the failure criterion for fiber failure is:

$$f_f = \sqrt{\left(\frac{\sigma_1}{\sigma_{1,\max}}\right)^2} \qquad (8)$$

$\sigma_{1,\max}$ *maximum stress in fiber direction (tension/compression).*

f_f *failure occurs when $f_f > 1$.*

And the damage parameter for fiber damage is:

$$d_f = \frac{1}{f_f} e^{\left(-\sigma_{1,\max}(f_f-1)/(C_{11}\,G_c)\right)} \qquad (9)$$

An orthotropic delamination model, describing mixed mode delamination, is applied. The delamination model has been implemented in the ABAQUS FE program, using the surface-to-surface contact option. In case of surface-to-surface contact, the FE meshes of adjacent plies do not need to be identical. The contact algorithm of ABAQUS will determine which node of the master surface is in contact with a given node on the slave surface.
components.

The user-subroutine UINTER can be used to specify a dedicated relation between the relative displacement and the corresponding traction forces. Hence, the user can define the interaction between the two surfaces.

Failure in this model is defined by:

$$f = \left(\left(\frac{u_1}{u_{1,\max}}\right)^\alpha + \left(\frac{u_2}{u_{2,\max}}\right)^\alpha + \left(\frac{u_3}{u_{3,\max}}\right)^\alpha\right)^{1/\alpha} \qquad (10)$$

α *constant (usually 2)*

u_1 *the normal direction of the master surface.*

u_2, u_3 *out-of-plane shear components.*

$u_{i,\max}$ *maximum displacements in the corresponding directions.*

f   *failure occurs when* *f* > 1.

Riveting

The analysis of bonded and riveted joints for FML is performed on the same approximation level. Therefore the concept of microscopic skin models is maintained and expanded to fasteners as well as particular overlapping geometries in FML, like splices. Micro-mechanical modelling of splices is quite similar to the approach presented for the undisturbed FML, the main difference is that gaps and additional resin-rich zones in the overlapping area have to be considered.

Despite the similarities, the numerical effort for the simulation of riveted joints is significantly higher: the rivet fastening is analysed by the use of an explicit integration scheme whilst a more simplified approximation with a contact fit option is used for the following implicit analysis of the external loading in order to save computation time.

By the help of this simplification, FE micro-models of lap joints have been built (see figure 12).
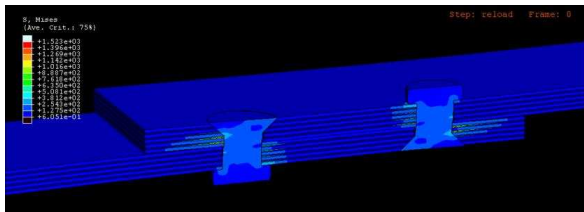
Figure 12. FE model of a riveted lap joint.

5 Results and Discussion

In this chapter a few results of the DIALFAST program are presented. In each picture the test results and the numerical results are presented simultaneously.

Mode I

The first picture (figure 13) gives the results for Mode I fracture energy testing of GLARE-3 at Room Temperture. The test results show some scatter, although for other series the scatter has been less, for others more. The numerical result (thicker blue line) in this particular plot matches

the experimental results very well. The numerical results of all Mode I Fracture Energy tests are in good agreement with the experimental results. The only deviations encountered sometimes are regarding the stiffness of the specimen.
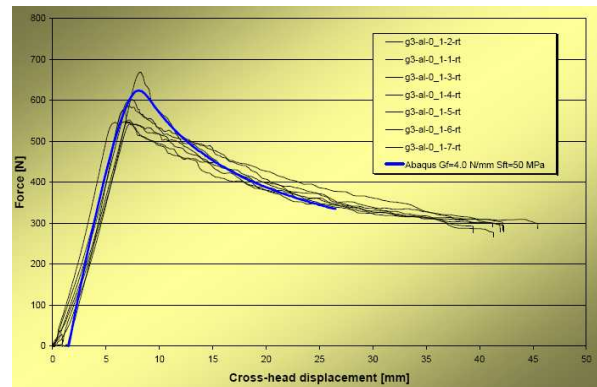
Figure 13. Test and numerical results for Mode I Fracture Energy testing of GLARE-3 at RT.

Mixed Mode

The second example of the fracture energy tests is a plot about the Mixed Mode testing of GLARE-3 at 80^0C. The ratio of the mode mix is 1 (or 50/50).

Again the agreement with the experimental results is good (see figure 14). In this particular case the numerical result underestimates the real test results a little.
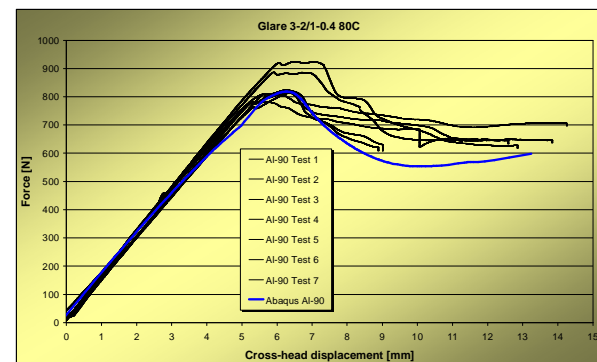
Figure 14. Test and numerical results for Mixed Mode Fracture Energy testing of GLARE-3 at 80^0 C.

Rivet strength

The last example presented in this paper is the failure of an anti-symmetric riveted lap joint. In

figure 15 a cross-section of such a joint is compared: an experimental result at the top and a numerical result below. When the deformations in the sections are compared qualitative agreement is very good.
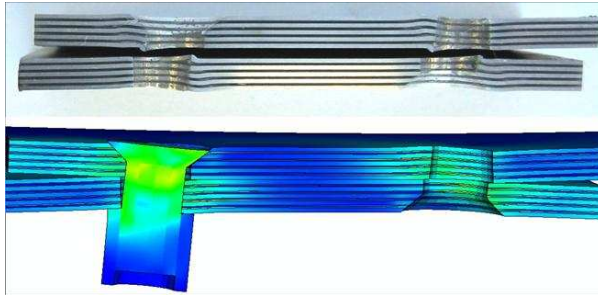
Figure 15. Cross sections of failed riveted joints: experiment (top), numerical (bottom)

A second picture of the riveted joints is presented in Figure 16. In this plot the test and numerical results are assembled of rivet strength tests; mark the unloading and reloading loop for the determination of the bearing yield strength. Again the agreement between the numerical (red line) and empirical results is very good.
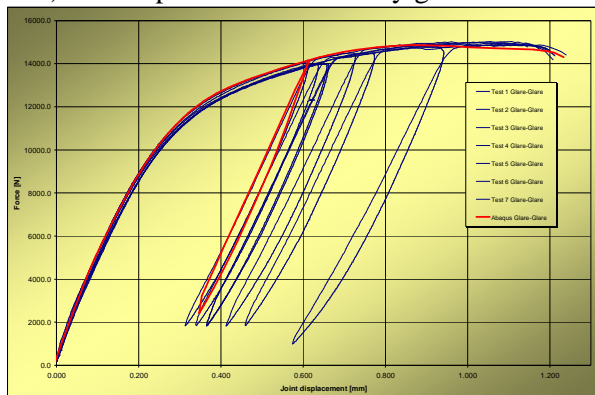
Figure 16. Rivet strength test data.

6 Conclusions

The conclusions from the results as presented in this paper are:
- the developed models can be applied to a wide range of FML materials (although in this paper only test results of GLARE-3 are presented).
- the developed micro-models are capable of predicting the most important damage mehanisms in FML
- the fracture energy analysis is a requirement for the analysis of failure at meso-scale.
- the models developed could be applied successfully for simulating rivet strength tests.
- there is a good agreement between the experimental and numerical results.

References

[1] DIALFAST – Development of Innovative and Advanced Laminates for Future Aircraft Structures, CEC 6th Framework Program, Specific Targeted Research Project No. 502846 (2004-2007).
[2] Vlot, A., *GLARE, History of the Development of a New Aircraft Material*, Kluwer Academic Publishers, the Netherlands, 2001
[3] Hagenbeek, M., *Characterization of FML under thermo-mechanical loadings*, PhD thesis, the Netherlands, 2005
[4] Rooijen van, R., *Bearing characteristics of Standard and Steel reinforced GLARE,* PhD thesis, the Netherlands, 2006
[5] Alderliesten, R.C., *Fatigue Crack Propagation and Delamination Growth in Glare*, PhD-thesis, The Netherlands, 2005
[6] Middendorf, P., Linde, P., Boer, H. de, Sinke, J., *Micro-mechanical modeling approach for Fiber Metal Laminates*, NAFEMS Conference, 2005.
[7] Vlot, A; Gunnink, J W – *Fiber Metal Laminates - An introduction,* Kluwer Academic Publishers, 2001
[8] Alessandrini, A., *Delamination Behaviour of Z-pinned Laminates under Shear Loading*, M.Sc. Thesis, Cranfield University, 2003